Towards Visual-Fatigue-Free BCI with Imperceptible Visual Evoked Potentials (I-VEP)

Milán András Fodor, and Ivan Volosyak

***Abstract*— A Brain–computer interface (BCI) enables direct control of external devices through neural activity. Among BCI paradigms, visual evoked potentials (VEPs) are widely used because they harness the brain's response to visual stimuli to deliver an intuitive and inclusive control interface. However, these systems typically rely on low-frequency flickering stimuli to evoke strong neural responses, which can cause discomfort and fatigue. While previous attempts have sought to mitigate this discomfort, eliminating it entirely would be ideal. This could be achieved with high-frequency flickering operating above the critical fusion frequency threshold, which is invisible to the human eye yet still evokes a distinct neural imprint. While this neural response is distinguishable from that of a non-flickering stimulus, reliably differentiating between two different high-frequency stimuli remains challenging.**

Our novel Imperceptible VEP (I-VEP) paradigm combines imperceptible high-frequency flicker segments with static (non-flickering) intervals to create patterns analogous to steady-state VEP (SSVEP) and code-modulated VEP (cVEP). From this paradigm, we define two variants: Imperceptible Steady-State VEP (I-SSVEP) and Imperceptible Code-Modulated VEP (I-cVEP). Our initial I-cVEP experiments demonstrate its feasibility, achieving a mean bit-wise accuracy of over 92% across 27 participants. These findings may represent a significant first step toward fully comfortable visual-stimulus BCIs, enabling broader adoption and improved usability.

I. INTRODUCTION

Brain-computer interfaces (BCIs) establish a direct pathway between brain activity and external devices [1]. They have gained significant interest for restoring motor function, enabling communication in severe paralysis, and enhancing human-computer interaction. Non-invasive systems, particularly those based on electroencephalography (EEG), are increasingly accessible, although challenges in reliability, usability, and real-world deployment persist [2].

Among various BCI paradigms, event-related potentials (ERPs) are widely employed because they directly measure brain responses associated with specific sensory, cognitive, or motor events. A key subclass, visual evoked potentials (VEPs), are neural responses elicited by visual stimuli. VEP-based BCIs leverage these signals to infer user intent, such as identifying gaze direction on a screen. Compared to other paradigms, VEP-based systems offer a high information transfer rate (ITR), intuitive use, and support for numerous commands, making them especially attractive for assistive communication [3].

Faculty of Technology and Bionics, Rhine-Waal University of Applied Sciences, 47533 Kleve, Germany

Faculty of Informatics and Data Science, Graduate School for Applied Research in North Rhine-Westphalia (PK NRW), 44801 Bochum, Germany
ivan.volosyak@hochschule-rhein-waal.de

In SSVEP paradigms, visual stimuli are presented at specific frequencies, typically between 5 and 40 Hz. When individuals fixate on these stimuli, synchronized neural responses emerge, producing periodic EEG patterns that can be reliably detected [4]. In contrast, cVEP paradigms use predefined sequences, such as binary m-sequences [5], to create rapid alternations (e.g., black and white frames at 60 Hz). These cyclic flickering patterns generate distinct neural responses identifiable in EEG signals [6].

Despite their effectiveness, VEP-based BCIs have a major drawback: visual discomfort. Strong, decodable VEPs require rapid, high-contrast changes, typically delivered via black-and-white flickering at 5–40 Hz. Such stimuli are often fatiguing, visually straining, and carry an increased epilepsy risk, significantly limiting their usability and broader acceptance [7], [8].

Various strategies have been explored to reduce the visual discomfort inherent in VEP-based BCIs. Researchers have employed high flickering frequencies [9], high duty-cycle stimuli [10], chaotic stimulation patterns [11], amplitude modifications [12], lower contrast levels [3], luminance modulation [13], personalized flicker frequencies [14], leveraging peripheral vision [15], novel monitor technologies [16], and alternative visual elements such as motion [13] or spatial grid patterns [17], among other approaches [7]. These methods aim to elicit the necessary visual responses with minimal discomfort.

Nonetheless, rapid perceptible changes—whether in contrast, position, or motion—continue to induce fatigue [7], [8]. An ideal VEP-based BCI could therefore elicit neural responses without any noticeable visual changes. This can be achieved with imperceptible flicker at frequencies above the critical flicker fusion (CFF) threshold—the perceptual boundary between a flickering and a steady light, which serves as a psychophysical measure of visual temporal resolution. However, the CFF is not a fixed value; it is known to vary with stimulus properties like luminance and size, and as a recent large-cohort study by Haarlem et al. demonstrated, it also varies substantially between individuals. They reported a 95% prediction interval of approximately 21 Hz around a mean of roughly 50 Hz, depending on the measurement method [18]. This high-frequency stimulation approach, known as Rapid Invisible Frequency Tagging (RIFT), still produces measurable neural imprints in EEG signals [19], [20].

Research on SSVEPs at or above the CFF remains sparse, largely because existing studies often exhibit limited flexibility and reduced decoding performance [21]. For example,

Jiang et al.'s four-target speller using phase modulation achieved an ITR of 16.73 bits per minute (bpm) [22], while Ming et al. later reached 52 bpm with spatial modulation—albeit with added visual irritation and scalability issues. Another study combined frequencies between 55–62.8 Hz with slight phase modulation to develop a 40-target BCI, yielding an ITR of 51.6 bpm [21]. However, at frequencies below 60 Hz, stimuli often still produce perceptible flicker, and overall performance remains lower than that of traditional visible SSVEP [4] and especially, that of cVEP-based spellers [6].

The fundamental challenge is that differentiating multiple high-frequency stimuli is inherently difficult due to limited neural discriminability [19]. Researchers have addressed this either by using frequencies below the CFF or by the use of additional modulation techniques (e.g., phase or spatial modulation) to improve differentiation, yet these methods have not produced flexible, high-performance VEP-based BCIs. Consequently, genuinely imperceptible and user-friendly stimuli remain uncommon.

This study introduces a novel paradigm—Imperceptible Visual Evoked Potentials (I-VEP)—which alternates imperceptible high-frequency flicker with static image intervals. To our knowledge, this is the first approach to generate complex neural response patterns by leveraging the binary contrast between a single high frequency flickering state and a static state. By adapting traditional code-modulated (cVEP) and steady-state (SSVEP) paradigms, our I-cVEP and I-SSVEP variants aim to deliver an imperceptible stimuli that remain just as decodable and scalable as their visible counterparts.

The primary objective of this study is to assess the practical feasibility of the I-cVEP paradigm by evaluating the neural discriminability of the proposed stimulus patterns and identifying optimal alternation frequencies and durations. If successful, this approach could overcome visual discomfort commonly associated with existing visual BCI systems, thereby enhancing usability and significantly broadening their application.

II. MATERIALS & METHODS

A. Experimental Procedure

Twenty-seven participants (15 females, 12 males; mean age 25.89 ± 4.96 years) provided written informed consent for this study, which was conducted in accordance with the Declaration of Helsinki and approved by the ethics committee of the medical faculty of Duisburg-Essen University (24-11957-BO). Participants could withdraw at any time and received €20 as compensation.

The experiment was conducted in the BCI laboratory at Rhine-Waal University of Applied Sciences. After completing a pre-questionnaire, participants undertook four experimental phases. During each phase, they focused on one visual target at a time. Stimuli appeared as gray boxes, either static or flickering at a high frequency, achieved through rapid alternation between maximum and minimum brightness levels. This resulted in a perceptually uniform gray tone, as depicted in Fig. 1. The static gray level was set once—prior to data collection—to RGB (180, 180, 180) based on an initial subjective calibration. The exact stimulus parameters varied by target and phase as follows:

- **Phase 0 – High-Frequency Flicker Rating:** For one round, participants rated perceived color change and discomfort for six conditions (static and flickering at 37.5, 45, 60, 90, and 180 Hz) on a 1–6 Likert scale. Each trial comprised a 3 s stimulus presentation followed by a questionnaire pause.
- **Phase 1 – Imperceptible Flicker Test:** EEG data were recorded over six rounds (3 s stimulus, 2 s pause) using the same six conditions from Phase 0, resulting in 36 trials total (6 conditions $\times$ 6 rounds).
- **Phase 2.A – I-cVEP (Slower):** For this phase, participants completed 18 trials (3 targets $\times$ 6 rounds). In each trial, a 60 Hz flicker encoded the binary '1' and a static frame encoded '0' for a 15-bit m-sequence (1,0,1,0,1,1,0,0,1,1,0,1,0,1,1). The sequence was presented twice per trial at 30 frames/bit, corresponding to a bit duration of $\approx$83 ms on the 360 Hz monitor. While subsequent targets were intended to use shifted sequences as best practice, a technical misstep resulted in the same sequence being used for all. TThis does not impair ta bit-wise decoding classifier,and random circular time-shifts during preprocessing was also applied so the model learns to classify each bit regardless of its absolute position.
- **Phase 2.B – I-cVEP (Faster):** In this phase, 24 trials were completed (3 targets $\times$ 8 rounds). Each trial displayed a 31-bit m-sequence (1,0,1,1,0,1,0,0,1,0,1,1,0,0,1,1,0,1,1,0,1,0,1,0,1,1,0,1,0,0,1) at a faster rate of 15 frames/bit ($\approx$42 ms bit duration).
- **Phase 3 – I-SSVEP:** In six rounds, stimuli alternated between 60 Hz flicker and a static display using these frame-ratio $\rightarrow$ alternation-rate pairs: 90/90 frames $\rightarrow$ 2 Hz, 60/60 $\rightarrow$ 3 Hz, 30/30 $\rightarrow$ 6 Hz, 15/15 $\rightarrow$ 12 Hz, 12/12 $\rightarrow$ 15 Hz, and a 33% duty-cycle condition of 15/30 $\rightarrow$ 8 Hz. Due to scope limitations, the analysis of this phase is reserved for future work.

B. Hardware and Software

Participants were seated approximately 80 cm from the monitor and instructed to minimize movement. EEG was recorded using a 16-channel g.USBamp amplifier (Guger Technologies, Schiedlberg, Austria) at a 1200 Hz sampling rate, with Ag/AgCl electrodes mounted on a standard EEG cap (EasyCap, 82237 Wörthsee, Germany) positioned according to the 10–5 system (P7, P3, Pz, P4, P8, PO7, PO3, POz, PO4, PO8, O1, Oz, O2, O9, Iz, O10). Electrode impedance was kept below 5 kΩ, referenced to Cz and grounded at AFz. Stimuli were presented on an Acer Nitro monitor (set to: 1920$\times$1080 pixels, 360 Hz vertical refresh rate, V-sync on, and otherwise default settings) connected to a Dell Precision Desktop (Intel i9-10900K CPU, NVIDIA RTX 3070/4070 Ti, Windows 10 Education). Neural network training used an NVIDIA RTX 4070 Ti GPU and AMD Ryzen 9 7950X3D CPU under Windows 11 Education.

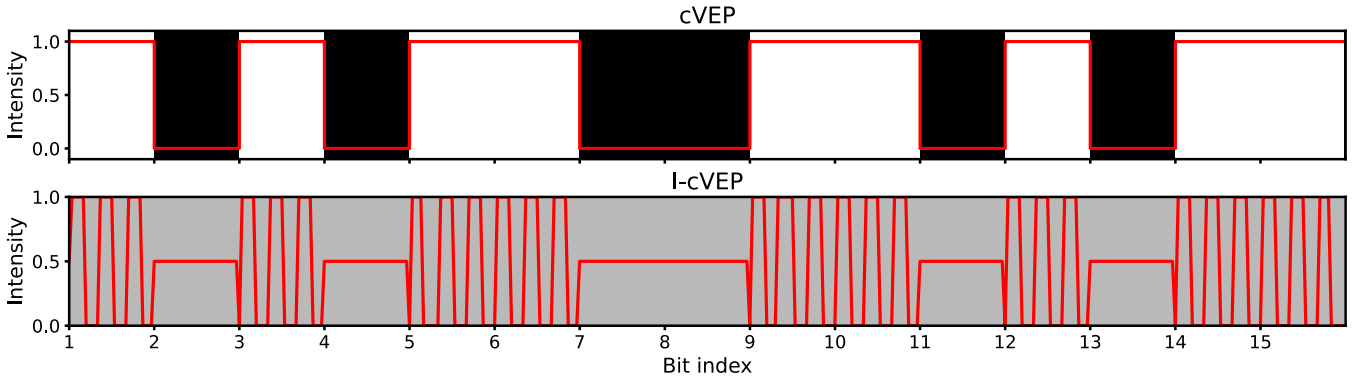

Fig. 1. Comparison of the cVEP and I-cVEP paradigms. The red graph illustrates the relative intensity for each bit of the stimulus, with '1' corresponding to maximum (white), '0' to minimum (black), and '0.5' to gray. By representing binary bit '1' as high-frequency flickering and bit '0' as a steady gray state, the I-VEP paradigm maintains a visually constant gray appearance while preserving the binary encoding of the stimulus.

Software environment for statistical analysis, plotting and neural network training included Python 3.9.13, TensorFlow 2.10.1, Spektral 1.3.1, Scikit-learn 1.6.1, SciPy 1.13.1, and NumPy 1.26.4, Matplotlib 3.9.4. Visual stimuli were implemented in Unity 2022.3.46f1 and presented to participants while synchronized EEG was recorded using the SNAP Brain Toolbox v2.2.8.1 (SNAP, Bochum, Germany). Requirements, scripts and full implementation details are available at: `https://github.com/MILANIUSZ/I-VEP`.

C. Evaluation

a) Phase 0: Subjective Ratings: Perceived color change and visual discomfort for each stimulus condition were rated on a six-point Likert scale (1 = none, 6 = extreme), and the mean scores were calculated.

b) Phase 1: EEG Power Analysis: To rank the carrier frequencies by their evoked neural response, we performed a power spectral analysis. For each 3-second trial, a 0.5-second sliding window moved across the data in 0.1-second steps. For each window, we used Welch's method to calculate the signal power in a narrow band (target frequency ± 1 Hz) for each of the 16 EEG channels. The mean of these power values across all channels was taken as a single feature point. This process yielded a distribution of power values for each stimulus condition, pooled across all participants, which was then used for visualization.

c) Phase 2: I-cVEP Decoding: To assess the decodability of the I-cVEP paradigm, we developed two distinct classification pipelines: a subject-specific classical machine learning baseline and a subject-agnostic deep learning model.

1) Offline Signal Decodability Baseline (SVC): To first validate that the I-VEP paradigm produces a fundamentally decodable signal, we implemented an offline analysis assuming known stimulus bit boundaries. Data from a 4-channel midline occipital-parietal montage (Pz, POz, Oz, Iz) was processed. After applying a 50 Hz notch filter, signal envelopes were extracted using the Hilbert transform across multiple frequency bands: narrow-band (60/120 Hz), broadband, and low-frequency (e.g., alpha/beta). This core power information was augmented with derived features, including trial-normalized power to counter signal drift, differential 'flip potentials' to detect transient responses at bit transitions, and a feature encoding the bit's temporal position within the trial. The resulting 12-feature set was standardized and used to train a Support Vector Classification (SVC) model with an RBF kernel. Performance was evaluated for each participant using a strict Leave-One-Trial-Out (LOTO) cross-validation scheme to produce a subject-specific bit-wise accuracy.

2) Subject-Agnostic Decoding (ResNet-CNN): Our primary decoding pipeline employs a bit-wise classification strategy, echoing other neural network-based modern c-VEP classifiers [23], but is uniquely tailored to the I-VEP signal. Rather than using an end-to-end model on raw EEG, our approach prioritizes targeted feature engineering to isolate the 60 Hz flicker signature. This allows the use of a relatively simple ResNet architecture focused on robustly classifying the presence of these pre-extracted features.

Preprocessing and Feature Engineering. The raw 1200 Hz EEG data was first downsampled to 240 Hz using a one-sided FIR filter (decimation factor of 5). This rate preserves an integer number of samples for each stimulus bit (10 samples for the 41.7 ms bits in Phase 2.B; 20 samples for the 83.3 ms bits in Phase 2.A). To promote generalization and invariance to a bit's absolute position, each trial segment was randomly time-shifted by a fraction of a bit's duration. Subsequently, two parallel, causal Butterworth filters isolated the 60 Hz carrier and its 120 Hz harmonic. The Hilbert transform was then applied to each band to extract its instantaneous amplitude (envelope) and unwrapped phase. Concatenating the amplitude and phase from both frequency bands resulted in a feature vector with four values per EEG channel at each time step. This feature-rich signal was then segmented into overlapping windows for classification.

Model Architecture. The network receives the windowed feature vectors, which first pass through a batch normalization layer. The core of the model is a single residual block comprising two 1D convolutional layers (32 filters each) with causal padding. Each convolutional layer is followed by batch normalization and a ReLU activation. A skip connection adds the block's input to its output before a

final ReLU activation. This is followed by max pooling, spatial dropout, a dense layer (64 units) with ReLU activation and dropout, and a final 2-unit softmax layer for binary classification.

Hyperparameter Optimization and Evaluation. To obtain an unbiased estimate of generalization performance, we employed a nested cross-validation (NCV) framework across the 27 participants, with a 4-fold subject-stratified outer loop. For each fold, an inner loop performed 50 Optuna trials (using a TPE sampler and Median Pruner) to fine-tune the selected range of hyperparameters on an 80/20% split of the training files. The search space for signal processing included: 4th or 5th-order Butterworth filter center frequencies ({59.8, 60.06, 60.3} Hz for fundamental; {119.6, 121.26, 122.0} Hz for harmonic), bandwidths (1.5–3 Hz), and a latency shift to align the label with the neural response (40–110 ms). The search also optimized architectural parameters like window size (167–250 ms), kernel size (46–63 ms), and channel selection (a focused 8-channel occipital set vs. all 16 channels). Training was performed with the AdamW optimizer, tuning the learning rate (3e-4 or 5e-4), ℓ_2 regularization (3e-6 or 1e-5), and dropout (0.2–0.3). A batch size of 64 was used, with class weights to handle any potential slight imbalance and early stopping (patience 10–15) on the validation loss to prevent overfitting. After identifying the best hyperparameters for a given fold, a final model was trained on all inner-loop data and evaluated on the held-out test set. The model's stride was set to match the bit length, and the resulting softmax probabilities were then thresholded at 0.5 to reconstruct the sequence and calculate bit-wise accuracy.

III. RESULTS

Data was recorded from 30 participants for the study. However, due to technical errors during data acquisition, the recordings of three participants were excluded. This resulted in a final cohort of 27 participants for analysis (15 females, 12 males; mean age 25.89 ± 4.96 years). Among this cohort, 77.77% reported prior BCI experience, and 37.37% required visual correction. The average tiredness rating was 2.46 (1 = not tired at all, 6 = very tired), with participants reporting an average of 6.78 hours of sleep.

TABLE I

MEAN LIKERT-SCALE (1–6) RATINGS (N = 27) FOR PERCEIVED COLOR CHANGE AND DISCOMFORT AT GIVEN FREQUENCIES, WHERE 6 DENOTES VERY DISCOMFORTING AND HIGHLY NOTICEABLE COLOR CHANGE.

	0 Hz	**37.5 Hz**	**45 Hz**	**60 Hz**	**90 Hz**	**180 Hz**
Noticeable color change	1.11	5.18	4.40	3.22	2.00	2.33
Discomfort	1.28	2.50	1.89	1.50	1.28	1.28

Phase 0 results were obtained using a Likert-scale questionnaire assessing perceived color change and discomfort for various flicker frequencies. Table I summarizes these ratings. The data indicate that lower flicker frequencies were associated with more noticeable color changes compared to the static (0 Hz) and higher frequency conditions, the same tendency was visible for discomfort as well.

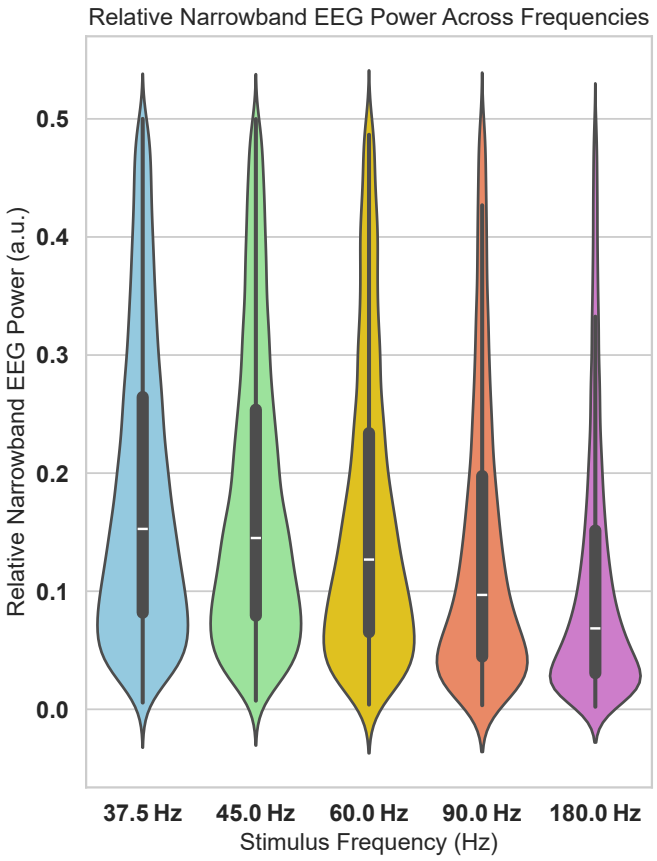

Fig. 2. Violin plot of narrowband EEG power (a.u.) across stimulus frequencies. Power was computed using Welch's method (± 1 Hz) on 0.5-second sliding windows and pooled across all 27 participants. The y-axis shows the mean power across all 16 channels for each window. Inner boxplots indicate the median and IQR of the distributions. Lower frequencies yield higher median power and broader distributions, reflecting a more robust response.

Phase 1 results are summarized in Fig. 2, which displays the distribution of narrowband EEG power pooled from all 27 participants across the five flicker frequencies. The data clearly shows that lower frequencies elicit stronger neural responses. The 37.5 Hz condition yielded a median power of 0.1528 a.u. (interquartile range [IQR] = 0.1826), approximately double the median power of 0.0685 a.u. (IQR = 0.1208) observed at 180 Hz.

TABLE II

I-CVEP DECODING PERFORMANCE. RESNET-CNN METRICS SHOW SUBJECT-AGNOSTIC PERFORMANCE (MEAN & STD. DEV. OVER 4 NCV FOLDS). THE SVC IS A SUBJECT-SPECIFIC BASELINE (MEAN & STD. DEV. OVER 27 SUBJECTS VIA LOTO). ALL ACCURACIES ARE REPORTED AT THE BIT-LEVEL.

Phase	**Decoder**	**Scheme**	**Acc (%)**	**Sd (%)**
2.B	SVC	LOTO	91.99	1.92
2.A	ResNet-CNN	4-fold CV	92.94	1.95
2.B	ResNet-CNN	4-fold CV	92.27	2.95

The performance of our I-cVEP decoding pipelines is sum-

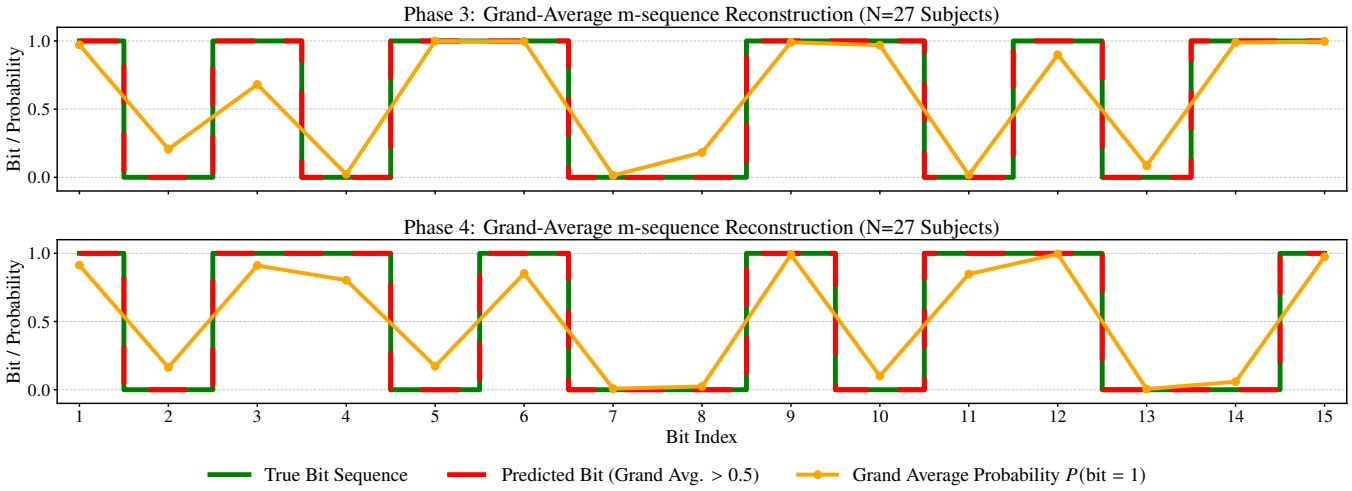

Fig. 3. Grand-average m-sequence reconstruction across all 27 participants. The final predicted bit (red dashed line) is derived by applying a 0.5 decision threshold to the grand-average softmax probability (orange line), shown against the ground-truth sequence (green line).
Top (Phase 2.A): Reconstruction of the 15-bit sequence. **Bottom (Phase 2.B):** Reconstruction of the first 15 bits of the 31-bit sequence.

marized in Table II. The offline SVC, serving as a subject-specific baseline, was tested only on the faster stimulus paradigm (Phase 2.B) and achieved a mean bit-wise accuracy of 91.99% ($\pm$1.92%).

Subsequently, the subject-agnostic ResNet-CNN decoder was evaluated on both paradigms. It demonstrated slightly higher performance, achieving a mean bit-wise accuracy of 92.94% ($\pm$1.95%) for the slower stimulus (Phase 2.A). Performance remained robust for the faster stimulus (Phase 2.B), with an accuracy of 92.27% ($\pm$2.95%). The high fidelity of this decoding is visually represented by the grand-average sequence reconstruction shown in Fig. 3.

IV. DISCUSSION

The questionnaire results confirm a key success of the I-VEP paradigm: stimulation at 60 Hz and above induced negligible visual discomfort (mean Likert ratings $\leq$ 1.50). However, a subset of participants reported a slight color shift even at the highest frequencies. This is likely not due to the perception of the high-frequency flicker itself, but rather a subtle mismatch between the time-averaged luminance of the flickering segments and the separately defined static gray. This observation highlights two priorities for future work. First, an automated, display-specific luminance calibration routine should be developed to perfectly match the perceived gray levels. Second, while we selected 60 Hz as a trade-off between robust signal strength (Fig. 2) and user comfort (Table I), exploring even higher carrier frequencies (e.g., 90 Hz) could further enhance perceptual uniformity. This is particularly relevant given recent findings of rare but significant individual variations in CFF, with some thresholds being around the 60 Hz mark, which could account for the few participants perceiving the actual a flicker-related effect in our study [18]. It is also possible that personal adjsutmetns are needed as the sahde of grey might be slightly different based on the persona ldiffernces teh rpeception of the high frequcnies, nonteh less these are the icign on the cake .

The results from our decoding analysis provide compelling evidence for the feasibility of the I-cVEP paradigm. As shown in Table II, our subject-agnostic ResNet-CNN achieved a mean bit-wise accuracy of 92.94% for the slower paradigm and a robust 92.27% for the faster one. This high level of accuracy is visualized in Fig. 3, where the grand-average reconstructed sequence closely tracks the ground truth, demonstrating a clear and consistent neural response to the imperceptible stimuli.

Given that our model employs causal filtering and a computationally efficient architecture, the I-cVEP pipeline is inherently suitable for real-time deployment. The prospect of online use is promising because the final target identification accuracy in a cVEP-BCI system often exceeds the underlying bit-wise accuracy. In an online system, the bit-wise decoded sequence is correlated against a set of known, circularly-shifted m-sequences. Due to the unique autocorrelation properties of these sequences, the correct target can often be identified with high confidence even if a few bits are decoded incorrectly. This suggests that if a similar level of performance can be maintained in an online setting, our high offline bit-wise accuracies could translate to even more reliable real-time control. The optimal 89 ms latency shift identified during hyperparameter optimization, combined with a 250 ms data window and the model's sub-millisecond inference time, suggests that a real-time system could achieve classification approximately 340 ms after bit onset.

A significant advantage demonstrated here is the model's subject-agnostic nature. Unlike traditional cVEP, where complex and user-specific response templates are often required, the I-VEP approach appears to elicit a more uniform neural response across individuals. This consistency, likely driven by the universal detection of the 60 Hz carrier, enables a single, generalized model to perform effectively for all users without calibration, which is a significant step towards user-friendly, plug-and-play BCIs. The ultimate potential

of I-VEP might be realized by incorporating additional modulation strategies—such as frequency, phase, or spatial modulation—to further increase the uniqueness of the neural responses. This could make the decoding process even more stable, especially for a high number of targets.

V. CONCLUSION

Our evaluation across a sizable participant cohort confirms that the proposed I-cVEP paradigm—alternating imperceptible high-frequency flicker with static intervals—produces a neural signal that can be reliably decoded from EEG. This approach induces little to no visual fatigue while following the same fundamental logic as a conventional cVEP-BCI, making it a good candidate as a more user-friendly alternative.

Looking ahead, we will assess the online performance of I-cVEP and compare it directly with that of traditional cVEP systems, both in terms of performance and user-friendliness. We will also analyze our I-SSVEP data to test its viability. Developing an automated luminance-matching routine will be a priority to realize a fully imperceptible paradigm, alongside further refining the decoding pipeline. The ultimate goal is to deploy this paradigm in a high-performance, multi-target online BCI, leveraging additional modulation strategies to achieve truly fatigue-free visual control for everyday assistive and interactive applications.

ACKNOWLEDGMENT

This work was supported by the European Union's research and innovation programme under the Marie Skłodowska-Curie grant agreement No 101118964. The authors thank "The Friends of the University Rhine-Waal - Campus Cleve" association for financial support. Additionally, we appreciate the contributions of student assistants and participants.

REFERENCES

[1] J. R. Wolpaw, J. del R. Millán, and N. F. Ramsey, "Chapter 2 – Brain–computer interfaces: Definitions and principles," in *Brain-Computer Interfaces*, *Handbook of Clinical Neurology*, vol. 168, pp. 15–23, 2020. [Online]. Available: 10.1016/b978-0-444-63934-9.00002-0

[2] C. Guger, J. M. Azorin, M. Korostenskaja, and B. Z. Allison, "Brain–Computer Interface Research: A State–of–the–Art Summary 12," in *Brain–Computer Interface Research*, Springer Nature Switzerland, 2025, pp. 1–10. [Online]. 10.1007/978-3-031-80497-7_1

[3] H. Xu, S.-H. Hsu, M. Nakanishi, Y. Lin, T.-P. Jung, and G. Cauwenberghs, "Stimulus Design for Visual Evoked Potential Based Brain-Computer Interfaces," *IEEE Transactions on Neural Systems and Rehabilitation Engineering*, vol. 31, pp. 2545–2551, 2023. [Online]. 10.1109/TNSRE.2023.3280081

[4] M. Li, D. He, C. Li, and S. Qi, "Brain-computer interface speller based on steady-state visual evoked potential: A review focusing on the stimulus paradigm and performance," *Brain Sciences*, vol. 11, no. 4, p. 450, Apr. 2021. [Online]. 10.3390/brainsci11040450

[5] E. E. Sutter, "The brain response interface: Communication through visually-induced electrical brain responses," *Journal of Microcomputer Applications*, vol. 15, no. 1, pp. 31–45, Jan. 1992. [Online]. 10.1016/0745-7138(92)90045-7

[6] V. Martínez-Cagigal, J. Thielen, E. Santamaría-Vázquez, S. Pérez-Velasco, and P. Desain, "Brain-computer interfaces based on code-modulated visual evoked potentials (c-VEP): A literature review," *Journal of Neural Engineering*, vol. 18, no. 6, p. 061002, Nov. 2021. [Online]. 10.1088/1741-2552/ac38cf

[7] M. Azadi Moghadam and A. Maleki, "Fatigue factors and fatigue indices in SSVEP-based brain-computer interfaces: A systematic review and meta-analysis," *Frontiers in Human Neuroscience*, vol. 17, Nov. 2023. [Online]. 10.3389/fnhum.2023.1248474

[8] T. Mu and Y. K. Lin, "Optimization of SSVEP-BCI interface design — A study based on visual comfort," in *Communications in Computer and Information Science*, 2024, pp. 138–144. [Online]. 10.1007/978-3-031-78516-0_14

[9] X. Chen, B. Liu, Y. Wang, H. Cui, J. Dong, R. Ma, N. Li, and X. Gao, "Optimizing stimulus frequency ranges for building a high-rate high frequency SSVEP-BCI," *IEEE Transactions on Neural Systems and Rehabilitation Engineering*, vol. 31, pp. 1277–1286, 2023. [Online]. 10.1109/TNSRE.2023.3243786

[10] J. Meng, H. Liu, Q. Wu, H. Zhou, W. Shi, L. Meng, M. Xu, and D. Ming, "A SSVEP-Based Brain–Computer Interface With Low-Pixel Density of Stimuli," *IEEE Transactions on Neural Systems and Rehabilitation Engineering*, vol. 31, pp. 4439–4448, 2023, 10.1109/TNSRE.2023.3328917

[11] Z. Shirzhiyan, A. Keihani, M. Farahi, E. Shamsi, M. GolMohammadi, A. Mahnam, M. R. Haidari, and A. H. Jafari, "Toward new modalities in VEP-based BCI applications using dynamical stimuli: Introducing quasi-periodic and chaotic VEP-based BCI," *Frontiers in Neuroscience*, vol. 14, Nov. 2020. [Online]. 10.3389/fnins.2020.534619

[12] S. Ladouce, L. Darmet, J. J. Torre Tresols, S. Velut, G. Ferraro, and F. Dehais, "Improving user experience of SSVEP BCI through low amplitude depth and high frequency stimuli design," *Scientific Reports*, vol. 12, no. 1, 2022. [Online]. 10.1038/s41598-022-12733-0

[13] M. Li, X. Chen, and H. Cui, "A high-frequency SSVEP-BCI system based on simultaneous modulation of luminance and motion using intermodulation frequencies," *IEEE Transactions on Neural Systems and Rehabilitation Engineering*, vol. 31, pp. 2603–2611, 2023. [Online]. 10.1109/TNSRE.2023.3281416

[14] S. Kondo and H. Tanaka, "High-frequency SSVEP-BCI with less flickering sensation using personalization of stimulus frequency," *Artificial Life and Robotics*, Aug. 2023. [Online]. 10.1007/s10015-023-00893-9

[15] X. Zhao, Z. Wang, M. Zhang, and H. Hu, "A comfortable steady state visual evoked potential stimulation paradigm using peripheral vision," *Journal of Neural Engineering*, vol. 18, no. 5, p. 056021, Apr. 2021. [Online]. 10.1088/1741-2552/abf397

[16] H. Maymandi, J. L. P. Benitez, F. J. Gallegos-Funes, and J. Pérez-Benítez, "A novel monitor for practical brain-computer interface applications based on visual evoked potential," *Brain-Computer Interfaces*, vol. 8, no. 1–2, pp. 1–13, 2021. [Online]. 10.1080/2326263x.2021.1900032

[17] G. Ming, H. Zhong, W. Pei, X. Gao, and Y. Wang, "A new grid stimulus with subtle flicker perception for user-friendly SSVEP-based BCIs," *Journal of Neural Engineering*, vol. 20, no. 2, p. 026010, 2023. [Online]. 10.1088/1741-2552/acbee0

[18] C. S. Haarlem, R. G. O'Connell, K. J. Mitchell, and A. L. Jackson, "The speed of sight: individual variation in critical flicker fusion thresholds," *PLOS One*, vol. 19, no. 4, pp. e0298007, 2024. [Online]. 10.1371/journal.pone.0298007

[19] C. S. Herrmann, "Human EEG responses to 1–100 Hz flicker: Resonance phenomena in visual cortex and their potential correlation to cognitive phenomena," *Experimental Brain Research*, vol. 137, no. 3–4, pp. 346–353, Apr. 2001. 10.1007/s002210100682

[20] M. Brickwedde, Y. Bezsudnova, A. Kowalczyk, O. Jensen, and A. Zhigalov, "Application of rapid invisible frequency tagging for brain computer interfaces," *Journal of Neuroscience Methods*, vol. 382, p. 109726, 2022. [Online]. 10.1016/j.jneumeth.2022.109726

[21] K. Liu, Z. Yao, L. Zheng, Q. Wei, W. Pei, X. Gao, and Y. Wang, "A high-frequency SSVEP-BCI system based on a 360 Hz refresh rate," *Journal of Neural Engineering*, vol. 20, no. 4, p. 046042, Aug. 2023. [Online] 10.1088/1741-2552/acf242

[22] L. Jiang, W. Pei, and Y. Wang, "A user-friendly SSVEP-based BCI using imperceptible phase-coded flickers at 60Hz," *China Communications*, vol. 19, no. 2, pp. 1–14, 2022. [Online]. 10.23919/JCC.2022.02.001

[23] Y. Dong, L. Zheng, W. Pei, X. Gao, and Y. Wang, "A 240-target VEP-based BCI system employing narrow-band random sequences," *Journal of Neural Engineering*, vol. 22, no. 2, pp. 026024, 2025. [Online]. 10.1088/1741-2552/adbfc1